

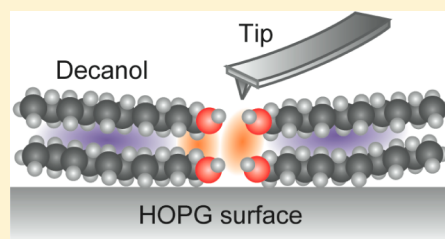
# Cross-Sectional Structure of Liquid 1-Decanol over Graphite

Takumi Hiasa,\* Kenjiro Kimura, and Hiroshi Onishi

Department of Chemistry, Graduate School of Science, Kobe University, 1-1 Rokko-dai, Nada, Kobe 657-8501, Japan

## S Supporting Information

**ABSTRACT:** The interface of graphite and liquid 1-decanol was studied using frequency modulation atomic force microscopy (FM-AFM). The topography of epitaxially physisorbed decanol on the substrate was traced with submolecular resolution. The tip–surface force was monitored in the liquid as a function of the vertical and lateral tip coordinates to reveal the cross-sectional structure of the interfacial decanol. Four or more liquid layers were identified by vertically modulated force distributions. The first and second liquid layers were laterally heterogeneous, as evidenced by a force distribution that was periodically modulated along lateral coordinates. A possible structuring mechanism is proposed on the basis of energy gain by hydrogen bonding and van der Waals interactions.



## 1. INTRODUCTION

The behavior of liquid at liquid–solid interfaces has received great attention from a broad range of fields such as chemistry, biology, and material sciences.<sup>1</sup> Surface tension and wettability are sensitive to structured liquid at interfaces. Likewise, protein stability and enzyme reactivity are thought to be controlled by interfacial water structured at these surfaces. However, our knowledge about how interfacial liquids are structured is limited.

The structuring mechanism is expected to be sensitive to intermolecular forces across the interface and within the liquid. The hydrogen bond interactions are dominant among functional groups capable of hydrogen bonding, while van der Waals forces are dominant among inert alkyl moieties. In a recent study, we showed that liquid water was hydrogen-bonded with surfaces to present laterally heterogeneous, site-specific structures on OH-terminated and COOH-terminated thiolate monolayers.<sup>2</sup> Site-specific structuring of interfacial water was also found on hydrophilic mica surfaces.<sup>3,4</sup> However, liquid hydrocarbons formed laterally uniform, layered structures over graphite<sup>5–12</sup> and CH<sub>3</sub>-terminated thiolate monolayers,<sup>13–15</sup> governed by van der Waals forces.

In the current study, we examined liquid 1-decanol on graphite. All-trans decanol is epitaxially physisorbed with the molecular axis parallel to the surface.<sup>16</sup> The hydrogen bonding capable OH and the alkyl chain of physisorbed decanol were exposed to liquid decanol. The decanol-covered graphite thus provided a surface patterned on a submolecular scale with the two contrasting moieties. The major point of contention here is how decanol liquid structures itself over this chemically heterogeneous surface.

Scanning tunneling microscopy (STM) has been used successfully in the in situ characterization of long-chain hydrocarbons and their derivatives physisorbed on graphite.<sup>16–19</sup> Atomic force microscopy (AFM) has the ability to observe liquid aliphatic alcohol layered on graphite, as reported in the literature.<sup>9,12,20–24</sup> When the force on the AFM tip is

measured as a function of the tip–surface distance, the layered density distribution of the liquid is projected onto the force–distance curves. Hofbauer et al.<sup>24</sup> reported force–distance curves modulated by layered dodecanol on graphite together with the molecularly resolved topography of physisorbed dodecanol. However, the lateral structure of liquid decanol layers still remains to be determined. We have applied advanced frequency-modulation AFM (FM-AFM)<sup>25</sup> with a 10 pN order force sensitivity to observe the cross-sectional force distributions of decanol-covered graphite.

## 2. EXPERIMENTAL SECTION

Highly oriented pyrolytic graphite (10 × 10 × 1.2 mm<sup>3</sup>, ZYA Quality, NT-MDT) was used as a substrate. Approximately 30  $\mu$ L of liquid 1-decanol (Wako, >97%) was dropped onto a freshly cleaved surface. A modified Shimadzu SPM 9600 microscope was operated using silicon cantilevers backside-coated with aluminum (NCH-R, Nanosensors). The nominal spring constant, resonance frequency, and quality factor of resonance were 40 N m<sup>−1</sup>, 130–150 kHz, and 5 in liquid decanol, respectively. The absolute cantilever deflection was calibrated using the theoretical amplitude of the thermal Brownian motion of the cantilever. The lateral displacement of the piezoelectric scanner was calibrated on mica and the vertical displacement on rutile TiO<sub>2</sub>(110). Imaging scans were carried out at room temperature.

## 3. RESULTS AND DISCUSSION

**3.1. Topography of Physisorbed Decanol.** The topography of decanol-covered graphite was traced by regulating the tip–surface distance to keep the resonance frequency shift of the cantilever oscillation ( $\Delta f$ ) constant. Results of the trace are shown in Figure 1. A typical large-area image is shown in

Received: October 16, 2012

Revised: November 27, 2012

Published: November 28, 2012

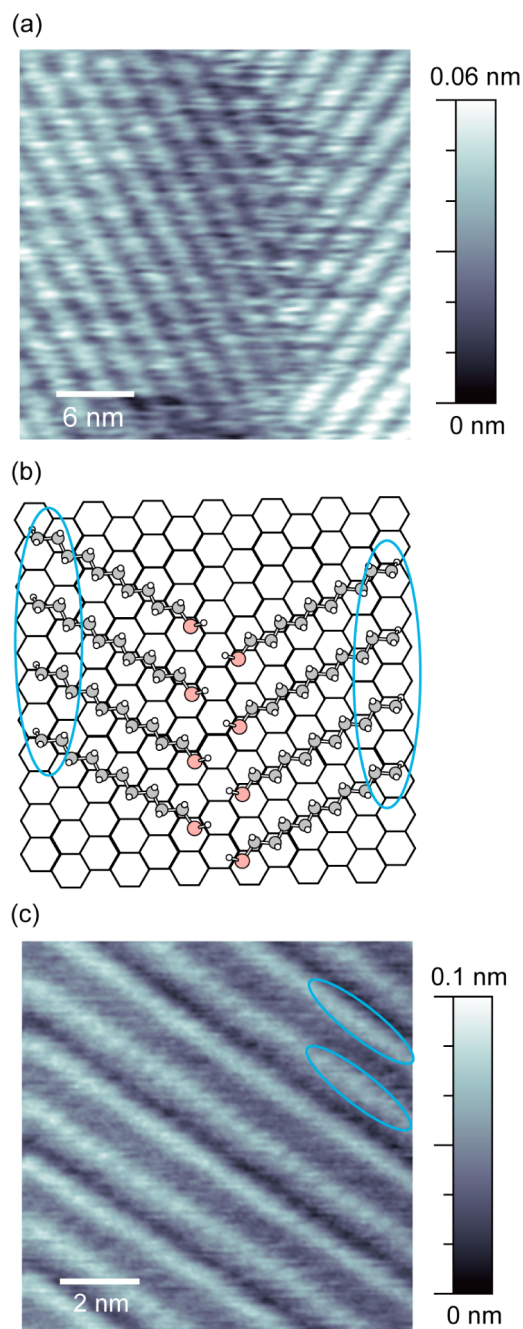


**Figure 1.** Decanol physisorbed on graphite. (a) Wide-area topography obtained at a frequency shift ( $\Delta f$ ) of +400 Hz. (b) The herringbone structure of the physisorbed layer drawn based on ref 29. Red spheres represent oxygen atoms. The lines of methyl terminals are marked by ovals. (c) Narrow-area topography obtained at a  $\Delta f$  set point of +300 Hz. Two bright edges are indicated by ovals. The cantilever oscillation amplitude in the topographic scans was 0.1 nm.

panel a. Columns of physisorbed decanol molecules are seen as stripes laterally separated by 2.6 nm. Some STM studies<sup>18,19</sup> showed that aliphatic alcohol molecules are paired via hydrogen bonding and that the paired molecules create columns that are epitaxial to the graphite lattice, as illustrated in panel b. The column width was found to be 2.65 nm using low-angle X-ray diffraction.<sup>26</sup> We found the column-to-column distance in our topography (a) to be consistent with the reported length. The column axis was epitaxial to the graphite substrate, as expected.<sup>27,28</sup> Two domains of different orientations are

encountered in the scanned area. The middle of the topography (a) was hollowed as little as 15 pm. This length is much smaller than the step height of graphite. Rearrangements of physisorbed decanol may be possible at the domain boundary.

Individual decanol molecules were resolved in the high-resolution topography shown in panel c. This is the appearance observed in repeated scans, though some different features appeared less frequently. In the major appearance of panel c, the edges of each column were terminated by a bright protrusion. A simulation predicted that physisorbed octadecanol could raise the terminal methyl away from the surface.<sup>19</sup> The protrusions can be assigned to the raised terminal part of physisorbed decanol. The spot seemed to be broadened compared to the size of the terminal methyl group. The convolution effect of the tip apex or some adjacent methylene groups lifted by the terminal methyl group may cause the broadening. One of the minor appearances is shown in the Supporting Information.

**3.2. Cross-Sectional Structure of Liquid Decanol.** In this subsection, we consider the structure of liquid decanol facing the physisorbed decanol columns. The structured liquid can be penetrated by the AFM tip; the tip–surface force is sensitive to the local density of the structured liquid. Cross-sectional distributions  $\Delta f$  were obtained in the following manner. The oscillating tip was scanned vertically from the bulk liquid toward the surface until  $\Delta f$  exceeded a threshold of +300 Hz. The threshold was tuned to be equal to the  $\Delta f$  set point employed in the topographic imaging shown in Figure 1c. Hence, the surface of the topography corresponds to the zero distance. The frequency shift was recorded as a function of the vertical coordinate. By repeating the vertical scans, a  $\Delta f$  distribution cross-sectional to the surface was constructed. A positive shift represents a repulsive force load on the tip, though the force strength is not directly proportional to  $\Delta f$ .

Figure 2 presents a  $\Delta f$  distribution over the decanol-covered surface shown in Figure 1. The distribution was determined along a plane perpendicular to the decanol column axis. A positive  $\Delta f$  shows up bright in the raw distribution in panel a. The vertical coordinate at which  $\Delta f$  reached the threshold was laterally modulated. The brightest region in the bottom of the image was accordingly corrugated and reproduced the topography observed in Figure 1.

Four dark layers appeared in the distribution. The alternate appearance of dark and bright layers signifies liquid structured along the vertical coordinate; four layers of liquid decanol laid over the physisorbed decanol columns. The first and second dark layers, as well as the bright layer between the two, are laterally modulated in brightness. This is a sign of a laterally heterogeneous density distribution of the layered decanol.

The  $\Delta f$ –distance curves obtained at topographic protrusions and grooves are shown in panel b. Curve (i) was collected on the physisorbed column marked by the vertical line (i) in panel a. Curve (ii) was collected on an interstitial position between adjacent columns. The two curves were modulated in a similar manner, with local maxima found at vertical distances of 0.5, 1.2, and 1.8 nm. The zero distance was defined to be the coordinate where  $\Delta f$  exceeded +300 Hz. The  $\Delta f$ –distance curve (i) was converted to a force–distance curve on the basis of Sader–Jarvis conversion<sup>30</sup> and shown in panel c. The force modulation amplitude was 30–10 pN in first, second, and third oscillations. The distance between first and second  $\Delta f$  maxima was determined on 128 of  $\Delta f$ –distance curves presented in panel a. A histogram of the first-to-second layer distances is available in Supporting Information, and the averaged distance

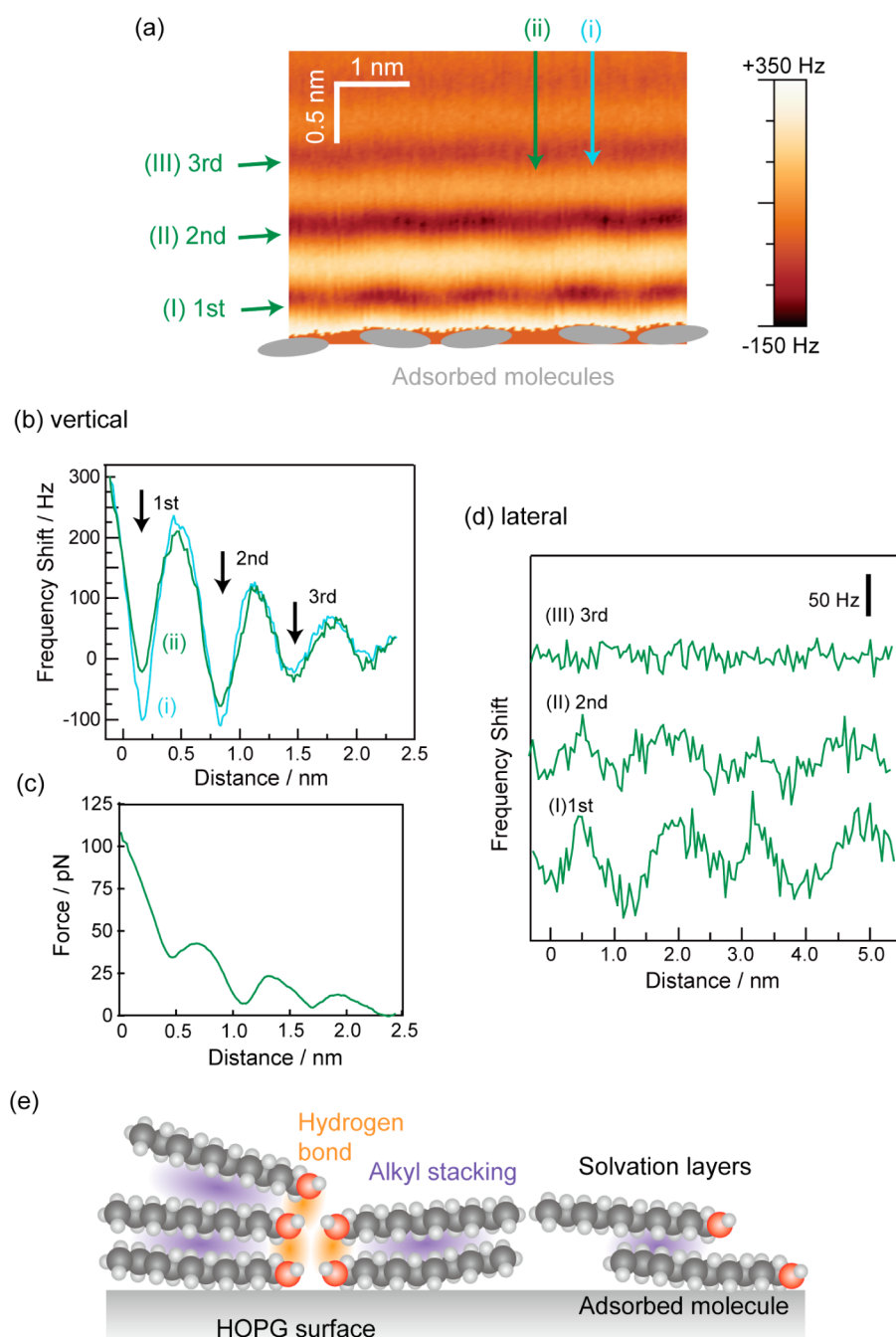


**Figure 2.** (a) Cross-sectional  $\Delta f$  distribution over the decanol-covered surface of Figure 1c. Cantilever oscillation amplitude: 0.1 nm. (b) Vertical  $\Delta f$ –distance curves obtained along lines (i) and (ii). (c) The force–distance curve converted from curve (i) in panel b. (d) Lateral  $\Delta f$ –distance curves obtained along the first, second, and third dark layers. (e) Schematic illustration of possible intermolecular interactions. The red and blue portions represent energy gain by the hydrogen bond and van der Waals interactions, respectively.

was 0.62 nm. The averaged distance is consistent with observations in previous AFM studies.<sup>9,12,21,24</sup> *n*-Alkanes of different chain lengths presented liquid layer distances of 0.6 nm on a  $\text{CH}_3$ -terminated thiolate monolayer,<sup>14</sup> suggesting flat lying alkanes. The distance of 0.62 nm similarly indicated flat lying decanol over graphite. Since the number of atoms in contact with neighboring molecules is maximized per molecule with a flat lying orientation, the potential energy is accordingly minimized due to van der Waals interaction of the physisorbed decanol and decanol in the first liquid layer. This should also be the case with decanol in the first and second liquid layers. The alternate dark and bright layers were the most visible features of

the distribution shown in Figure 2a. The major role played by van der Waals forces in constructing vertical structures of liquid decanol is thus suggested.

The first and second dark layers were modulated along the lateral coordinate. The  $\Delta f$ –distance curves of panel b showed different oscillation amplitudes. The amplitude from the first minimum to the first maximum was larger on curve (i) than on curve (ii). This was also the case with the second oscillation but not with the third oscillation. This is clearly shown by the lateral  $\Delta f$ –distance curves in panel d. The three curves were constructed from the first, second, and third dark layers along a coordinate parallel to the surface.



Here, we assume that a large  $\Delta f$  oscillation amplitude represents enhanced structuring of the liquid decanol. The large amplitudes on curve (i) indicate that liquid decanol preferred to be on top of a physisorbed decanol column rather than in an interstitial position between adjacent columns. A possible origin of this preference is hydrogen bonding. When liquid decanol is present on top of physisorbed decanol, the OH groups of the two molecules can form a hydrogen bond. An additional energy gain by van der Waals interaction is expected from the stacked alkyl chains. The decanol in the first liquid layer is positioned with the largest possible contact area with the adsorbed decanol in order to maximize the energy gain. The hydrogen bond would be broken and the van der Waals energy gain reduced if the liquid decanol was shifted away from the on-top position of the adsorbed column. This interpretation is illustrated in panel e. The third liquid layer was homogeneous along the lateral coordinate. The lateral heterogeneity in the layered liquid is induced by the physisorbed decanol columns via decanol–decanol interaction from the physisorbed to first liquid layer, from first to second liquid layer, and so on. The strength of the heterogeneity should reduce as a function of the vertical distance from the surface to the bulk decanol liquid. Our result in panel a showed that the heterogeneity strength of the third liquid layer was below the detection limit of the microscope.

Figure 3 presents wide-area  $\Delta f$  distributions on two planes; one perpendicular and the other nearly parallel to the decanol columns. The periodic corrugations induced by the columns are apparent at the bottom of distribution a, with a corrugation period of 1.3 nm. A laterally heterogeneous distribution was present in the first and second liquid layers, as seen in Figure 2. The distribution in Figure 3a was determined in a plane parallel to the plane of Figure 2. In distribution b, the lateral period of topographic corrugations was 5 nm because the plane was finitely tilted from the column axis. The first and second dark layers in the liquid were again present and laterally modulated at the column boundaries. The modulation period was accordingly increased to 5 nm. The coincident period is consistent with the potential energy barrier across the column boundary proposed in Figure 2e. The  $\Delta f$  distribution was homogeneous along the column axis suggesting a uniform potential energy surface in this direction. Even when decanol in the first liquid layer shifts from the on-top position of a physisorbed decanol, the hydrogen bond and the van der Waals interaction are still available. Decanol movements along the axis do not cost potential energy in the first liquid layer. However, decanol movements across a column boundary cause a loss of the hydrogen bond and van der Waals gain.

#### 4. CONCLUSIONS

A graphite wafer was immersed in liquid 1-decanol and probed using advanced FM-AFM. In topographic scans, epitaxially physisorbed decanol was structured in columns protruding from the surface. Four or more liquid layers were identified over the decanol-covered surface as vertically modulated distributions of the tip–surface force. A flat lying orientation of liquid decanol was evidenced by a layer-to-layer distance of 0.6 nm. The first and second liquid layers were laterally heterogeneous, as evidenced by force distributions periodically modulated along lateral coordinates. A potential energy barrier was proposed across the column boundaries of physisorbed decanol to interpret the observed lateral heterogeneities. Inefficient hydrogen bonding and van der Waals interactions can induce the barrier. The lateral heterogeneity present on the

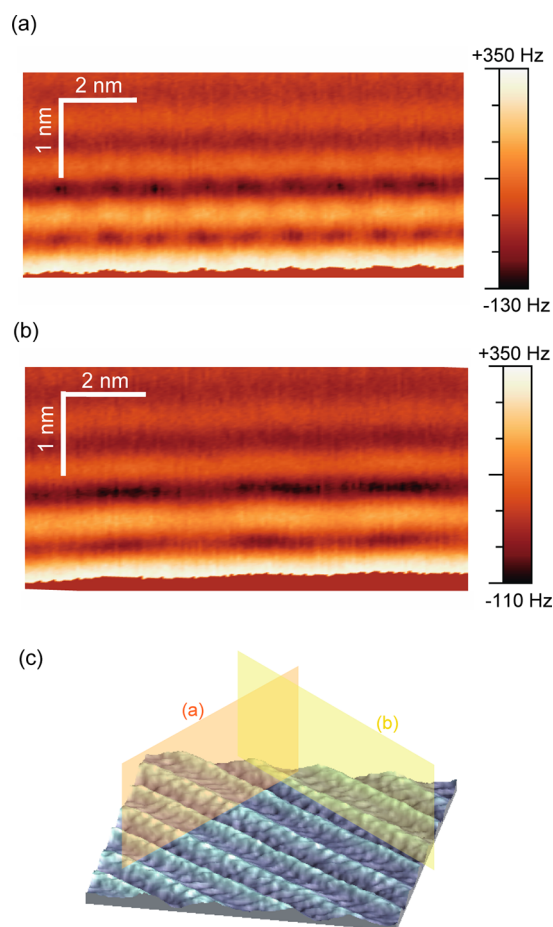


**Figure 3.** Cross-sectional  $\Delta f$  distributions (a) perpendicular and (b) nearly parallel to the physisorbed decanol column axis. Cantilever oscillation amplitude: 0.1 nm. (c) The azimuth of the two cross-sectional planes with a bird's-eye view of the decanol-covered surface.

decanol-covered surface was screened by two liquid decanol layers. The different decay lengths found for the lateral and vertical heterogeneity may be the result of the flat lying orientation of interfacial decanol.

#### ■ ASSOCIATED CONTENT

##### Supporting Information

Minor topographic appearance of the decanol-adsorbed surface and the statistical analysis of first-to-second liquid layer distance. This material is available free of charge via the Internet at <http://pubs.acs.org>.

#### ■ AUTHOR INFORMATION

##### Corresponding Author

\*E-mail: [hiasa@people.kobe-u.ac.jp](mailto:hiasa@people.kobe-u.ac.jp).

##### Notes

The authors declare no competing financial interest.

#### ■ ACKNOWLEDGMENTS

The microscope used in this study was developed by the Advanced Measurement and Analysis Project of the Japan Science Technology Agency in collaboration with Masahiro Ohta, Kazuyuki Watanabe, Ryohei Kokawa, Noriaki Oyabu, Kei Kobayashi, and Hirofumi Yamada. This work was supported by a Grant-in-Aid for Scientific Research on Priority Areas [477] "Molecular Science for Supra Functional Systems." T.H. was

supported by the Japan Society for the Promotion of Science Fellowship.

## ■ REFERENCES

- (1) Israelachvili, J. N. *Intermolecular and Surface Forces*; Academic Press: London, U.K., 2011.
- (2) Hiasa, T.; Kimura, K.; Onishi, H. *Phys. Chem. Chem. Phys.* **2012**, *14*, 8419–8424.
- (3) Kimura, K.; Ido, S.; Oyabu, N.; Kobayashi, K.; Hirata, Y.; Imai, T.; Yamada, H. *J. Chem. Phys.* **2010**, *132*, 194705.
- (4) Fukuma, T.; Ueda, Y.; Yoshioka, S.; Asakawa, H. *Phys. Rev. Lett.* **2010**, *104*, 016101.
- (5) Xia, T. K.; Landman, U. *Phys. Rev. B* **1993**, *48*, 11313–11316.
- (6) Klein, D. L.; McEuen, P. L. *Appl. Phys. Lett.* **1995**, *66*, 2478.
- (7) Lim, R.; O'Shea, S. J. *Phys. Rev. Lett.* **2002**, *88*, 246101.
- (8) Gosvami, N. N.; Sinha, S. K.; Hofbauer, W.; O'Shea, S. J. *J. Chem. Phys.* **2007**, *126*, 214708.
- (9) Lim, L. T. W.; Wee, A. T. S.; O'Shea, S. J. *Langmuir* **2008**, *24*, 2271–2273.
- (10) Gosvami, N. N.; Sinha, S. K.; O'Shea, S. J. *Phys. Rev. Lett.* **2008**, *100*, 076101.
- (11) Pham Van, L.; Kyrylyuk, V.; Polesel-Maris, J.; Thoyer, F.; Lubin, C.; Cousty, J. *Langmuir* **2009**, *25*, 639–642.
- (12) Beer, S.; Wennink, P.; van der Weide-Grevelink, M.; Mugele, F. *Langmuir* **2010**, *26*, 13245–13250.
- (13) Srivastava, P.; Chapman, W. G.; Laibinis, P. E. *Langmuir* **2005**, *21*, 12171–12178.
- (14) Hiasa, T.; Kimura, K.; Onishi, H. *Colloids Surf., A* **2012**, *396*, 203–207.
- (15) Hiasa, T.; Kimura, K.; Onishi, H. *Jpn. J. Appl. Phys.* **2012**, *51*, 025703.
- (16) Cyr, D. M.; Venkataraman, B.; Flynn, G. W. *Chem. Mater.* **1996**, *8*, 1600–1615.
- (17) Watel, G.; Thibaudau, F.; Cousty, J. *Surf. Sci.* **1993**, *281*, L297.
- (18) McGonigal, G. C.; Bernhardt, R. H.; Yeo, Y. H.; Thomson, D. J. *J. Vac. Sci. Technol., B* **1991**, *9*, 1107.
- (19) Miao, X.; Chen, C.; Zhou, J.; Deng, W. *Appl. Surf. Sci.* **2010**, *256*, 4647–4655.
- (20) O'Shea, S. J.; Welland, M. E.; Rayment, T. *Appl. Phys. Lett.* **1992**, *60*, 2356.
- (21) Nakada, T.; Miyashita, S.; Sazaki, G.; Komatsu, H.; Chernov, A. A. *Jpn. J. Appl. Phys.* **1996**, *35*, L52–L55.
- (22) O'Shea, S. J.; Welland, M. E. *Langmuir* **1998**, *14*, 4186–4197.
- (23) Franz, V.; Butt, H.-J. *J. Phys. Chem. B* **2002**, *106*, 1703–1708.
- (24) Hofbauer, W.; Ho, R. J.; Hairulnizam, R.; Gosvami, N. N.; O'Shea, S. J. *Phys. Rev. B* **2009**, *80*, 134104.
- (25) Fukuma, T.; Kimura, M.; Kobayashi, K.; Matsushige, K.; Yamada, H. *Rev. Sci. Instrum.* **2005**, *76*, 053704.
- (26) Morishige, K.; Takami, Y.; Yokota, Y. *Phys. Rev. B* **1993**, *48*, 8277–8281.
- (27) Venkataraman, B.; Breen, J. J.; Flynn, G. W. *J. Phys. Chem.* **1995**, *99*, 6608–6619.
- (28) Yang, T.; Berber, S.; Liu, J.-F.; Miller, G. P.; Tománek, D. *J. Chem. Phys.* **2008**, *128*, 124709.
- (29) Yin, S.; Wang, C.; Xu, Q.; Lei, S.; Wan, L.; Bai, C. *Chem. Phys. Lett.* **2001**, *348*, 321–328.
- (30) Sader, J. E.; Jarvis, S. P. *Appl. Phys. Lett.* **2004**, *84*, 1801.